

Manuscript Number:

Title: Polymer functionalized nanocomposites for metals removal from water and wastewater: an overview

Article Type: Review Article

Keywords: Polymer functionalized nano-composites; metalloid; metal; nanoparticles; removal efficiency; toxicity

Corresponding Author: Dr. Giovanni Libralato, Dr.

Corresponding Author's Institution: University Ca' Foscari Venice

First Author: Giusy Lofrano

Order of Authors: Giusy Lofrano; Maurizio Carotenuto; Giovanni Libralato, Dr.; Rute F Domingos; Arjen Markus; Luciana Dini; Ravindra K Guatam; Daniela Baldantoni; Marco Rossi; Sanjay K Sharma; Mahesh C Chattopadaya; Maurizio Giugni; Sureyya Meriç

Suggested Reviewers: Charlotte Hurel
maitre de conference, Université de Nice-Sophia Antipolis
Charlotte.HUREL@unice.fr
expertise in wastewater and nanomaterials

Giorgio Bertanza
professor, University of Brescia
giorgio.bertanza@unibs.it
expertise in wastewater management, adsorbents and membranes

Rosa Freitas
researcher, Departamento de Biologia & CESAM, Universidade de Aveiro
rosafreitas@ua.pt
expertise in ecotoxicity on nanomaterials and water management

Ioannis K Kalavrouziotis
professor, HELLENIC OPEN UNIVERSITY SCHOOL OF SCIENCE and TECHNOLOGY
ikalabro@eap.gr
expertise in wastewater management

Cover Letter

Dear Editor,

We would like to submit to **Water Research** the following paper:

Polymer functionalized nanocomposites for metals removal from water and wastewater: an overview

This review paper deals with **emerging nano-based technologies** for **metals** removal from wastewater as tertiary or quaternary treatment.

We reviewed and organised the existing information about polymer functionalized nanocomposites (PFNCs) about **metals/metalloids removal** evidencing the existing gaps into the knowledge about their composition, **effects related to pH, temperature, contact time with wastewater, adsorbent capacity compared to metals' concentration, and their regeneration and reuse**. Data were discussed evidencing how efficient the technology could be as well as the role of metal speciation, their toxicity as a whole and final consideration about PFNCs' design.

Pollution by metal and metalloid ions is one of the most widespread environmental concern. They are non-biodegradable, and, generally, present high water solubility facilitating their environmental mobilisation interacting with abiotic and biotic components such as adsorption onto natural colloids or even accumulation by living organisms, thus, threatening human health and ecosystems. Therefore, there is a high demand for effective removal treatments of heavy metals, making the application of adsorption materials such as PFNCs, increasingly attractive. PFNCs retain the inherent remarkable surface properties of nanoparticles, while the polymeric support materials provide high stability and processability. These nanoparticle-matrix materials are of great interest for metals and metalloids removal thanks to the functional groups of the polymeric matrixes that provide specific bindings to target pollutants. Despite the promises of these adsorbents, several issues related to their use still remain to be addressed:

- Safety for human health and the environment has not been fully assessed - further research is expected in the near future investigating the long term exposure and effects considering various biological targets;
- Greening the PFNCs production is expected in order to minimize the use of solvents and make their use more environmentally friendly;
- Removal efficiency and cost optimization per unit volume treated waiting for an economy of scale;
- Life cycle impact analysis according to the reuse, recovery and regeneration approaches and zero-waste perspective.

The authors state that there is no conflict of interest and agreed to the submission.

Highlights

- PFNCs incorporate NPs surface features and the polymers binding capacity
- The interest in PFNCs is increasing, but many gaps into the knowledge exist
- Interesting removal rates for metals/metalloids, but no data on toxicity effects

1 **Polymer functionalized nanocomposites for metals removal from water and wastewater: an**
2 **overview**

3 Giusy Lofrano^{1,2}, Maurizio Carotenuto¹, Giovanni Libralato^{3,*}, Rute F. Domingos⁴, Arjen
4 Markus⁵, Luciana Dini⁶, Ravindra Kumar Gautam⁷, Daniela Baldantoni¹, Marco Rossi⁸, Sanjay
5 K. Sharma⁹, Mahesh Chandra Chattopadaya⁷, Maurizio Giugni², Sureyya Meric¹⁰

6

7 ¹ Department of Chemistry and Biology, University of Salerno, Via Giovanni Paolo II 132,
8 84084 Fisciano (Salerno), Italy

9 ² Department of Environmental and Civil Engineering, University of Naples “Federico II”, Via
10 Claudio 21, 80127 Naples, Italy

11 ³ Department of Environmental Sciences, Informatics and Statistics, University Cà Foscari
12 Venice, Via Torino 155, 30170, Venice, Italy

13 ⁴ Institut de Physique du Globe de Paris, Sorbonne Paris Cité, Université Paris Diderot, UMR
14 CNRS 7154, 75238 Paris Cedex 05, France

15 ⁵ Deltares, PO Box 177, 2600 MH Delft, The Netherlands

16 ⁶ Department of Biological and Environmental Science and Technology, University of Salento
17 Prov.le Lecce-Monteroni, 73100 Lecce, Italy

18 ⁷ Environmental Chemistry Research Laboratory, Department of Chemistry, University of
19 Allahabad, Allahabad 211 002, India

20 ⁸ Dipartimento di Scienze di Base e Applicate per l'Ingegneria - Via Antonio Scarpa 14/16,

21 00161 Roma

22 ⁹ Green Chemistry & Sustainability Research Group, Department of Chemistry, JECRC

23 University, Jaipur-303905, India

24 ¹⁰Corlu Engineering Faculty, Environmental Engineering Department, Namık Kemal University,

25 Corlu 59860, Tekirdag, Turkey

26 ***Corresponding author**

27 Dr. Giovanni Libralato

28 Via Torino 155

29 30170 Venezia

30 Italy

31 email: giovanni.libralato@unive.it

32 Tel. +39 3498833526

33

34 **Abstract**

35 Pollution by metal and metalloid ions is one of the most widespread environmental concern.
36 They are non-biodegradable, and, generally, present high water solubility facilitating their
37 environmental mobilisation interacting with abiotic and biotic components such as adsorption
38 onto natural colloids or even accumulation by living organisms, thus, threatening human health
39 and ecosystems. Therefore, there is a high demand for effective removal treatments of heavy
40 metals, making the application of adsorption materials such as polymer-functionalized
41 nanocomposites (PFNCs), increasingly attractive. PFNCs retain the inherent remarkable surface
42 properties of nanoparticles, while the polymeric support materials provide high stability and
43 processability. These nanoparticle-matrix materials are of great interest for metals and metalloids
44 removal thanks to the functional groups of the polymeric matrixes that provide specific bindings
45 to target pollutants. This review discuss PFNCs synthesis, characterization and performance in
46 adsorption processes as well as the potential environmental risks and perspectives.

47

48 **Keywords**

49 Polymer functionalized nano-composites; metalloid; metal; nanoparticles; removal efficiency;
50 toxicity

51

52	Index	
53	1. Introduction.....	6
54	2. Synthesis and characterization of polymer functionalized nanocomposites.....	7
55	2.1 S-PFNCs.....	7
56	2.2 B-PFNCs	8
57	2.3 Characterization	10
58	3 Removal of metals by PFNCs.....	11
59	3.1 Adsorption isotherms	11
60	3.2 Effect of polymer matrix and NPs composition.....	12
61	3.3 Effect of pH.....	13
62	3.4 Effect of temperature and contact time	14
63	3.5 Effect of initial concentration of metal ions and adsorbent dose	14
64	3.7 Effect of coexisting ions.....	15
65	3.8 Regeneration and reuse	15
66	4. Discussion.....	16
67	4.1 Synthesis methods	16
68	4.2 Process efficiency.....	17
69	4.3 Metals dynamic speciation.....	18
70	4.4 Toxicity evaluation.....	19
71	4.5 Design considerations	21

72	5. Conclusions.....	24
73	6. References.....	27
74		

75 **1. Introduction**

76 As a consequence of the growing pressure on water supply, the use of unconventional water sources
77 such as treated wastewater will be a new norm, especially in historically water-stressed regions (Qu
78 et al., 2013). This has resulted in several technological innovations within the field of wastewater
79 treatment, including advanced oxidation processes, adsorption, and membrane separation (Grassi et
80 al., 2012; Carotenuto et al., 2014). However, the application of these technologies has been
81 restricted due to processing efficiencies, operational methods, energy requirements, and economic
82 benefit. A promising technological breakthrough is expected from the nanotechnology field, which
83 holds a great potential for advancing water and wastewater treatment with improved treatment
84 efficiency and lower energy consumption, being considered one of the largest engineering
85 innovations since the Industrial Revolution (Wang et al., 2013). Some applications utilize the
86 smoothly scalable size-dependent properties of nanoparticles (NPs) related to their high specific
87 surface area, such as fast dissolution, high reactivity, and strong sorption, whereas others take
88 advantage of their discontinuous properties, such as superparamagnetism, localized surface plasmon
89 resonance, and quantum confinement effects (Mahdavian and Mirrahimi, 2010; Qu et al., 2013).
90 The nano-size of particles may be of concern about mass transport and excessive pressure drops
91 when applied in fixed-bed or any other flow-through systems, as well as difficulties in separation
92 and reuse, and even possible risk to human health and the ecosystems caused by their potential
93 release into the environment (Zhao et al., 2011).

94 Polymer-functionalized nanocomposites (PFNCs) incorporate the remarkable features of both NPs
95 and polymers: the unique physical and chemical properties resulting from the large surface area to
96 volume ratios, the high interfacial reactivity of nanofillers, and outstanding mechanical properties
97 and compatibility owing to their polymer matrix (Pan et al., 2009; Zhao et al., 2011), being also
98 amenable to regeneration and reuse (Zhou et al., 2009; Nassar et al. 2010). These features made of a
99 promising class of adsorbent materials for metals removal from water and wastewater (Ghorbani

100 and Eisazadeh, 2013). The overall objective of this review focuses on the PFNCs synthesis,
101 characterization, toxicity, and adsorption performance, including a perspective of new research
102 trends.

103

104 **2. Synthesis and characterization of polymer functionalized nanocomposites**

105 In the last decades, several PFNCs have been fabricated for the adsorptive removal of heavy metals
106 from water and wastewater (DeMarco et al., 2003; Cumbal and Sengupta, 2005; Sylvester et al.,
107 2007; Pan et al., 2010). According to the formation processes, PFNCs can be fabricated by i)
108 grafting NPs into polymer structures, or ii) by anchoring polymers to NPs (Mahdavian and
109 Mirrahimi, 2010). As shown in Figure 1, two methods can be used for their fabrication: i) direct
110 compounding; and ii) *in situ* synthesis (Zhao et al., 2011). Depending on the host materials, they
111 can be classified as synthetic (S-PFNCs) and biopolymer (B-PFNCs) functionalized
112 nanocomposites. The synthesis processes of S-PFNCs and B-PFNCs as reported in literature are
113 shown in Table 1 and Table 2, respectively.

114

115 **2.1 S-PFNCs**

116 Polymeric ion exchangers can be positively or negatively charged (Figure 2). In a polymeric cation
117 exchanger, negatively charged sulfonic acid groups are covalently attached to the polymer chains,
118 usually polystyrene. Conversely, a polymeric anion exchanger contains a high concentration of non-
119 diffusible positively charged quaternary ammonium functional groups.

120 Among S-PFNCs, the polystyrene-sulfone, as a polymeric cation exchanger, represents the most
121 common host material used to fabricate hybrid adsorbents by grafting NPs into polymers (DeMarco
122 et al., 2003; Cumbal and Sengupta, 2005; Pan et al., 2006; Sylvester et al., 2007; Zhang et al., 2008;
123 Sarkar et al., 2011).

124 The selective sorption of these hybrid polymers toward heavy metals can be explained on the basis
125 of their specific structure including: i) the negatively charged host material, and ii) the highly
126 dispersion of the NPs onto the inner surface of the polymers. Such sorption preference is mainly
127 attributed to two mechanisms: i) Donnan's membrane effect caused by the negatively charged
128 supporting material, and ii) specific affinity between NPs and heavy metals.

129 Several NPs are used to fabricate this kind of PFNCs, most cases by *in situ* synthesis (Table 1).
130 Hydrated iron (III) oxide (HFO), which is innocuous, inexpensive, readily available, and chemically
131 stable over a wide pH range 2 - 8, is the most common NPs used to fabricate S-PFNCs, as shown in
132 Table 1.

133 Amino-functionalized materials are expected to be highly effective for the removal of heavy metals,
134 since the elimination of anionic metal species can be achieved via electrostatic interaction, ion
135 exchange or hydrogen bonding, whereas the removal of the cationic metal species can be performed
136 via coordination with the amino groups (Zhao et al., 2010; Shen et al., 2012).

137 The main drawback of this kind of granular type adsorbents is related to their recovery once
138 saturated and their potential inhomogeneous dispersion. A large variety of fibrous exchangers based
139 on different polymers has been synthesized and tested in different processes to overcome these
140 limitations (Vatutsina et al., 2007).

141

142 **2.2 B-PFNCs**

143 Several authors reported that magnetic NPs functionalized with biopolymers such as chitosan
144 (Chang and Chen, 2005) (Tran et al., 2010) (Zhou et al., 2009), alginate (Bée et al., 2011); Lim et
145 al., 2009), gum Arabic (Banerjee and Chen, 2007) and cellulose (Guo and Chen, 2005) Zhu et al.,
146 2011) are highly efficient for the removal of toxic metals from aqueous solutions. The main
147 advantages of using iron oxides as composite materials with host materials are the high porosity,
148 magnetic properties, and, usually, good settling properties. Since surface functional group reactions
149 are involved in the sorption processes, higher content of surface functional group sites in a sorbent

150 would lead to a higher sorption capacity for the removal of contaminants (Nah et al., 2006; Jin et al.
151 2007). Among biopolymers, chitosan represents a valuable alternative having great potential
152 applications in the areas of biotechnology for wastewater treatment. Chang and Chen (2005)
153 developed a novel B-PFNC by carboxy-methylated chitosan covalently bounded on the surface of
154 Fe_3O_4 NPs (Ch-(Fe_2O_3)), via *in situ* synthesis. Chitosan functionalization can be achieved by using
155 environmentally friendly reagents. Zhou et al. (2009) carried out the surface modification of
156 chitosan-coated magnetic NPs (Ch - ($\gamma\text{-Fe}_2\text{O}_3$)) with α -ketoglutaric acid (α -KA), which is a natural,
157 inexpensive, harmless and biological reagent containing active functional groups like carboxyl
158 groups. Physical characterization confirmed that the chitosan coating process did not alter
159 significantly the $\gamma\text{-Fe}_2\text{O}_3$ morphology and the superparamagnetic properties of the α -KA- Ch - (γ -
160 Fe_2O_3) did not change markedly after coating. Bée et al. (2011) developed a B-PFNC by
161 encapsulation of magnetic functionalized NPs in calcium-alginate beads (CA - ($\gamma\text{-Fe}_2\text{O}_3$)), one of
162 the main components of brown seaweed. The authors reported that the use of nanosized magnetic
163 material improves the adsorption capacity of the alginate beads because of their large surface area
164 and the presence of surface binding groups due to the citrate coating. As shown in Table 2, most B-
165 PFNCs were obtained by *in situ* synthesis, whereas the alginate based ones were produced via direct
166 compounding. A novel B-PFNC was also developed by Banerjee and Chen (2007) treating Fe_3O_4
167 NPs with gum Arabic (GA-(Fe_3O_4)). The surface modification did not result in the phase change of
168 Fe_3O_4 leading to the formation of secondary particles in the range of 13-67 nm. Spherical
169 Fe_3O_4 /bacterial cellulose (Ce-(Fe_3O_4)) B-PFNCs were biosynthesized from *Gluconacetobacter*
170 *xylinum* by agitation fermentation (Zhu et al., 2011). The ability of cyclodextrins (CDs), cyclic
171 oligosaccharides consisting of 6 (α), 7 (β), 8 (γ) glucopyranose units linked together via α (1-4)
172 linkages, to complex various metals was found to be highly dependent on the modification of the
173 CDs with suitable functional groups through esterification, oxidation reactions and cross-linking of
174 hydroxyls outside the interior cavity (Norkus, 2009). Carboxymethyl- β -cyclodextrin (C - β - CD)

175 polymer modified (C- β -CD- (Fe_3O_4)) presented the lowest diameter (8 nm) compared to the other
176 B-PFNCs (Badruddoza et al., 2011, 2012, 2013a).

177

178 **2.3 Characterization**

179 Various and complementary multiscale characterization techniques are required for the analysis of
180 structural, morphological and functional properties of PFNCs. The polymer nanocomposite
181 morphology is mainly investigated by a large variety of microscopy techniques, depending on the
182 scale of interest, and ranging from optical to electron microscopy (SEM and TEM, with related
183 diffraction techniques) and scanning probe microscopy (SPM). The development of nanocomposite
184 science and technology and the optimization of the functional properties of PFNCs has been
185 possible because of the unparalleled information gathered with the use of these techniques. The
186 information about morphology and structure achieved at the different scales regards not only the
187 structure and distribution of the filler itself, but also the filler-matrix adhesion, and how the
188 presence of the filler impacts on the embedding polymer matrix properties (Michler et al., 2008).

189 Currently, there is a growing interest focused on the use of specialized microscopy techniques such
190 as electron tomography and the low voltage approach due to their ability to provide quantitative
191 information about the adhesion and dispersion of the filler in the embedding polymeric matrix
192 (Khare and Burris 2010). When *in situ* investigations are applicable and possible, specific
193 information can be obtained on the filler matrix interaction properties thus increasing the
194 comprehension of the mechanisms behind the characteristics enhancement observed for
195 nanocomposites. Other commonly and widely used characterization tools are: i) X-ray diffraction
196 (XRD) for the structural analysis, ii) Fourier Transform Infrared (FTIR) and Raman spectroscopy,
197 for the study of the modes of surface groups and the nature of chemical bonds, iii) thermal analysis
198 for the determination of water uptake, and iv) ionic exchange capacity.

199

200 **3 Removal of metals by PFNCs**

201 The basic principle for the use of PFNCs for metals removal is adsorption. Overall, various effects
202 contribute determining the whole efficacy of PFNCs action.

203

204 **3.1 Adsorption isotherms**

205 The investigation of the interactions between adsorbate and adsorbent showed that adsorption
206 isotherms are the most significant. Adsorption isotherms are functional expressions that correlate
207 the amount of solute adsorbed per unit weight of the adsorbent and the concentration of the
208 adsorbate in the bulk solution at a given temperature under equilibrium conditions. The isotherms
209 based on Langmuir (Langmuir, 1918) (Eq. 1) and Freundlich (Freundlich, 1906) (Eq. 2) approaches
210 are the most widely used to describe the equilibrium sorption of metal ions:

$$211 \quad \frac{C_e}{q_e} = \frac{C_e}{q_m} + \frac{1}{q_m K_L} \quad (\text{Eq. 1})$$

$$212 \quad \ln q_e = \left(\frac{1}{n}\right) \ln C_e + \ln K_L \quad \ln q_e = \left(\frac{1}{n}\right) \ln C_e + \ln K_L \quad (\text{Eq. 2})$$

213 In Eq. 1, q_e is the amount of adsorbate adsorbed per mass of adsorbent at equilibrium (mg g^{-1}), C_e is
214 the equilibrium concentration of adsorbate in aqueous solution (mg L^{-1}), q_m is the monolayer
215 adsorption capacity at equilibrium (mg g^{-1}) and K_L the Langmuir equilibrium constant. In Eq. 2, K_F
216 is an index of adsorption capacity, and n is the Freundlich constant (index of adsorption intensity or
217 surface heterogeneity). The Freundlich model assumes adsorption can occur in multiple layer, so
218 that saturation cannot occur, whereas the Langmuir model assumes adsorption occurs in only one
219 layer. Therefore the Langmuir constant represents the monolayer saturation at equilibrium.

220 To determine whether the adsorption is favourable, a dimensionless constant separation factor or
221 equilibrium parameter R_L is defined based on Eq. 3 (Weber and Chakravorti, 1974):

$$222 \quad R_L = \frac{1}{1 + K_L C_i} \quad (\text{Eq. 3})$$

223 where, C_i (mg L^{-1}) is the initial metal concentration, and R_L value indicates whether the type of the
224 isotherm is favourable ($0 < R_L < 1$), unfavourable ($R_L > 1$), linear ($R_L = 1$), or irreversible ($R_L = 0$).
225 Badruddoza et al. (2013) reported R_L values between 0 and 1 for the Langmuir isotherm, and
226 Freundlich adsorption intensity variables (n values) > 2 supporting the favourable adsorption of
227 metal ions by C- β -CD - (Fe_3O_4). R_L values also between 0 and 1 were determined for nano
228 magnetic polymer adsorbents coupled with different diamino groups for any initial concentration of
229 Cr(VI) (Zhao et al., 2010). For an initial concentration of Cr(VI) of 50 mg L^{-1} , the polymer nano-
230 adsorbents R_L values were 0.11, 0.04, 0.21, and 0.14 for EDA-(Fe_3O_4), DETA-(Fe_3O_4), TETA-
231 (Fe_3O_4) and TEPA-(Fe_3O_4), respectively. The adsorption isotherms followed the Langmuir rules.
232 The isotherm parameters are summarised in Table 3 and Table 4 for S-PFNCs and B-PFNCs,
233 respectively.

234

235 **3.2 Effect of polymer matrix and NPs composition**

236 Cumbal and Sengupta (2005) observed that, despite greater HFO content, the sorbents based on
237 cation-exchanger were practically unable to remove As(V) compared to the anion-exchanger based
238 sorbents. This phenomenon was explained by the Donnan exclusion effect, which is essentially an
239 extension of the second law of thermodynamics, concerning in a specific way the completely
240 ionized electrolytes in a heterogeneous system.

241 The magnetic properties of the composite materials and their possible result in higher adsorption
242 capacities towards metals is currently under discussion (Bibak, 1994). Davis and Bhatnagar, (1995)
243 have shown the ratio between the magnetic “core” and the “shell” plays an important role: i) a low
244 ratio of the magnetic oxide (the “core”) may cease a magnetic response, while ii) a low ratio of
245 polymer component (the “shell”) may lead to a decrease on the adsorption capacity.

246 The adsorption of Hg^{2+} by MP-(Fe_3O_4) seems to be highly related to the content of Fe_3O_4 magnetic
247 core in the adsorbents (Pan et al., 2012). The maximum adsorption capacity increased from 129.9
248 mg g^{-1} to 256.4 mg g^{-1} with an increase from 0 to 1.0 g of Fe_3O_4 used for the MP-(Fe_3O_4)

249 preparation, whereas a decrease from 256.4 mg g⁻¹ to 158.7 mg g⁻¹ was obtained when increasing
250 the Fe₃O₄ quantity from 1.0 g to 2.0 g. The optimized content of the magnetic core on the MP -
251 (Fe₃O₄) was 5.88% of Fe₃O₄. Similarly, the amount of iron as oxyhydroxide was also a crucial
252 factor for the arsenic adsorption capacity (Guo and Chen, 2005). Katsoyiannis and Zouboulis,
253 (2002) observed that the adsorption capacity of CPDB - (HFO) increased with an increasing amount
254 of coated iron oxide.

255

256 **3.3 Effect of pH**

257 The pH affects the functional groups deprotonation determining the strength of the complexation or
258 adsorption of the metals and metalloids. A first approach to evaluate the adsorption capacity of
259 adsorbents towards metals is the determination of the pH at the point of zero charge (PZC). The
260 overall surface charge on a PFNC becomes positive when the pH of the solution is below the PZC
261 inhibiting the approach of the positively charged metal ions (electrostatic repulsion) (Zhou et al.,
262 2009). Guo and Chen (2005) studied the influence of pH in the range (4-11) on the adsorption of
263 AsO₃³⁻ and AsO₄³⁻ (300 mg L⁻¹). In general, the removal rate of AsO₄³⁻ decreased with increasing
264 pH. The percentage removal of AsO₄³⁻ by Ce-(HFO) decreased from 96.2% to 52.6% when
265 changing the pH from 4 to 11. The percentage of AsO₃³⁻ removal by Ce-(HFO) was higher than that
266 for AsO₄³⁻ (90% for pH values between 5-10) except when pH was 4 – 5. Optimal AsO₃³⁻
267 adsorption by Ce-(HFO) was found at pH 7 – 9 where the percentage removed was above 95%
268 (Table 4).

269 The adsorption capacities of MP-(Fe₃O₄) for Hg²⁺ increased with increasing the pH, reaching a
270 steady-state at pH between 4 - 6 (Pan et al., 2012). This could be explained by the PZC of MP-
271 (Fe₃O₄) at pH 2.03 – 2.72, indicating that repulsion takes place when there is the presence of cations
272 such as Hg²⁺, HgOH⁺ and HgCl⁺, thus, resulting in low adsorption capacities at pH below 2.7.

273

274 **3.4 Effect of temperature and contact time**

275 Some studies (Chang and Chen, 2005; Badruddoza et al., 2011, 2012, 2013a) reported that the
276 adsorption capacity of metal ions decreases with increasing temperature, indicating that adsorption
277 is an exothermic process being the electrostatic interaction between metal ions and PFNCs lower at
278 higher temperatures. Also the contact time between the adsorbent and adsorbate is an important
279 parameter to design the adsorption processes.

280 The time at which the equilibrium is reached may drastically change depending on adsorption sites
281 on the exterior of the adsorbents: 100 min for Cd^{2+} , Cu^{2+} , and Pb^{2+} adsorption by D001 - (HFO)
282 (Pan et al., 2010), 240 min for Pb^{2+} adsorption by CA-($\gamma\text{-Fe}_2\text{O}_3$) Bée et al. (2011), 2 min for Cu^{2+}
283 adsorption rate by GA-(Fe_3O_4) (Banerjee and Chen 2007).

284

285 **3.5 Effect of initial concentration of metal ions and adsorbent dose**

286 Zhu et al., 2011 reported that when the concentrations of Mn^{2+} and Cr^{3+} were lower than 60 mg mL^{-1} ,
287 the adsorbed quantities on Ce-(Fe_3O_4) resulted proportional to their concentrations.

288 An optimum adsorbent dose is required to maximize the interactions between the metal ions and the
289 available adsorption sites on the adsorbent. Zhou et al. (2009) observed that the increase of Ch - ($\gamma\text{-}$
290 Fe_2O_3) from 0 to 7 g L^{-1} resulted in an increase of the Cu^{2+} removal efficiency (99%), whereas
291 higher concentrations lead to an adsorption decrease (Table 4). Evidently, that this effect is
292 dependent on external factors such as the stirring of the solution, in fact the increase of the PFNC
293 concentration with no change of the agitation speed can result in aggregation of the PFNC lowering
294 the availability of the functional groups for complexation of the metal ions. The solution ion
295 concentration drops to a lower value at higher adsorbent dose, and the system reaches equilibrium at
296 lower values of the concentration of adsorbed metal indicating that the adsorption sites remain
297 unsaturated.

298

299 **3.7 Effect of coexisting ions**

300 Coexisting ions in solution can compete with metals for the adsorption sites affecting the removal
301 process (Guo and Chen, 2005; Vatutsina et al., 2007; Pan et al., 2012). The major anionic
302 antagonistic components are phosphate (PO_4^{2-}), silicate (SiO_4^{4-}), and sulphate (SO_4^-), which are
303 usually present in groundwater streams. According to Katsoyiannis and Zouboulis (2002),
304 phosphate concentrations $< 50 \text{ mg L}^{-1}$ do not show any significant inhibition on As removal by
305 CPDB-(HFO), whereas for concentrations above 200 mg L^{-1} PO_4^{2-} strongly compete with As for the
306 available adsorption sites even impeding its removal when attaining concentrations of 400 mg L^{-1} .
307 When the presence of SiO_4^{4-} , the removal rate of AsO_3^{3-} decreases by Ce-(HFO) decrease to 85%,
308 but with less importance on the Ce-(HFO) adsorption when in presence of PO_4^{2-} (Guo and Chen,
309 2005).

310 The effect of Ca^{2+} , Mg^{2+} , and Na^+ on the adsorption of Hg^{2+} seems not to be significant since these
311 cations have less affinity to $-\text{SH}$ groups than Hg^{2+} as predicted by HSAB theory (Pan et al., 2012).

312

313 **3.8 Regeneration and reuse**

314 Hybrid ion exchangers can offer advantages over other adsorbents due to their chemical stability,
315 and durable physical structure and amenability to regeneration and reuse (Sarkar et al., 2011).
316 Regeneration of adsorbents has two main objectives: i) to restore the adsorption capacity of
317 exhausted adsorbents, and ii) to recover valuable metals present in the adsorbed phase. The first aim
318 can be attained under acidic conditions; the H^+ ions protonate the adsorbent surface, *i.e.*, the
319 carboxyl groups ($-\text{COOH}$), resulting in desorption of the positively charged metal ions (*i.e.*,
320 competition between the H^+ and the M^{Z+} for the $-\text{COO}^-$ groups).

321 The regeneration efficiency of Ch-($\gamma\text{-Fe}_2\text{O}_3$) was tested (Zhou et al., 2009) by using four different
322 eluents, Na_2EDTA , HCl , CH_3COOH and citric acid, at two different concentrations, 25 and 100
323 mmol L^{-1} . The obtained results showed that 100 mmol L^{-1} of Na_2EDTA have had the highest
324 efficiency (91.5%), due to its larger complexation capacity towards the metal ions. Yu et al. (2011)

325 showed the highest efficiency of Na₂EDTA to desorb Pb²⁺ ions when added to C-β-CD-(Fe₃O₄).
326 Also, Nassar et al. (2010) showed that HNO₃ and Na₂EDTA solutions have very high desorption
327 efficiencies for Pb²⁺ from CDpoly-MNPs (96.0 and 94.2% recovery, respectively), whereas H₃PO₄
328 was found to be a better eluent for Cd²⁺ and Ni²⁺ desorption (with a recovery of 61.8 and 82.7%,
329 respectively).

330 The desorption data of adsorbed Pb²⁺ ions from magnetic alginate beads by elution with 2 mol L⁻¹
331 HNO₃ showed that 88.9% of the Pb²⁺ ions were released in the solution after 30 min (Bée et al.,
332 2011). The adsorption capacity of the magsorbent was maintained at the same level even after 5
333 elution cycles, indicating that the magsorbent can be reused for the removal of heavy metals (Nassar
334 et al 2010).

335 Zhu et al. (2011) also showed that spherical Fe₃O₄/bacterial cellulose nanocomposites (Fe₃O₄/BC)
336 could be regenerated by using sodium citrate and reused for further adsorption of metals.

337

338

339

340

341 **4. Discussion**

342 **4.1 Synthesis methods**

343 The direct compounding process is more convenient for operation, it has a low cost and is suitable
344 for massive production (Katsoyiannis and Zouboulis, 2002). However, some drawbacks are related
345 to: i) the decision about the space distribution parameter of NPs on the polymer matrix, ii) the
346 possibility of NPs to form larger agglomerates during blending, greatly decreasing the advantages
347 of their nano-size dimensions, and iii) the polymer degradation upon melt compounding and phase
348 separation between the nano-phase and the polymer, which is sometimes severe (Zhao et al., 2011).

349 *In situ* synthesis methods allow synthesizing nanocomposites with tailored physical properties, and
350 with a direct and homogeneous dispersion of the NPs into the liquid monomers or precursors
351 avoiding their agglomeration in the polymer matrix, and thus improving the interfacial interactions
352 between both phases. However, use of solvents and/or catalysts can be necessary (Zhao et al.,
353 2011).

354

355 **4.2 Process efficiency**

356 As shown in Table 3, batch studies have shown that polymeric cation exchangers functionalized
357 with HFO NPs PS-(HFO) represent the most common option for arsenic removal due to the high
358 affinity of HFO for these metal ions (Etzel et al., 1997; De Marco et al., 2003; Cumbal et al., 2005;
359 Sylvester et al., 2007; Möller et al., 2008). However, by using ACP - N(CH₃)₂ - (HFO), removal of
360 approximately 90% of both AsO₃³⁻ and AsO₄³⁻ was obtained in only 10 min (Vatutsina et al.,
361 2007). Zouboulis et al. (2002) noted that the removal of arsenic was greatly affected by the
362 Fe(NO₃)₃ concentration used for the creation and doping of the iron oxide alginate beads. The
363 amounts of doped iron oxides were 2.8 and 1.4 mg of Fe/g of wet alginate bead, respectively. The
364 breakthrough point was reached after the treatment of around 80 and 55 bed volumes after the first
365 and second runs, respectively.

366 For the removal of Pb²⁺, Hg²⁺ and Cd²⁺ the use of PA-(HFO) showed a very high adsorption
367 potential, as shown in Table 3. PEI – NCs were also found highly efficient for Cr⁴⁺, Cu²⁺, Zn²⁺,
368 Cd²⁺, and Pb²⁺ removals. The use of PEI - (Fe₃O₄) + SiO₂ also produced high removal efficiencies
369 the order being: Cr⁶⁺ > Cu²⁺ > Zn²⁺ > Cd²⁺ with a starting concentration of 100 mg L⁻¹ (Pang et al.,
370 2011a, 2011b).

371 As shown in Table 4, Ch - (γ-Fe₂O₃) are also highly efficient (99%) for Cu²⁺ removal at pH > 2.
372 The adsorption rate equilibrium was achieved after 1 min due to the absence of internal diffusion
373 resistance.

374

375 4.3 Metals dynamic speciation

376 Metal complexation is often strongly pH dependent and a function of metal-binding affinity, ligand
377 concentration, and ionic strength (Domingos et al. 2015). Therefore, when the PNFCs are added to
378 an environmental compartment, either a wastewater treatment facility or a river, where metals are
379 present, these colloidal materials will absorb them through covalent, electrostatic, or hydrophobic
380 interactions. If these colloidal materials are not well stabilized, they in turn can undergo several
381 processes that are under dynamic control such as conformational changes of the organic colloids or
382 the electrical surface field on the inorganic colloids, which implies that there will be a kinetic
383 dependence on the metal complexation. These transformations result in a wider distribution of
384 complexation affinities for metals and metalloids, and, thus in a broader distribution of their
385 complex dissociation kinetics. In this case, the formed complexes can have different liabilities
386 (Herman et al., 2001): i) labile complexes - the kinetic flux is much larger than the diffusive one so
387 that the free metal ion will be in equilibrium with its complex forms all along the diffusion layer,
388 thus all metals present will contribute to the overall flux; and ii) non-labile complexes - the kinetic
389 and diffusive fluxes are of the same order of magnitude, thus both the free metal ion and a small
390 part of the bound metal will contribute to the overall flux. Evidently, this is of critical importance
391 for the evaluation of the removal efficiencies if the equilibrium is not attained. When no steady state
392 is achieved it is necessary to consider the distributions of both thermodynamic and kinetic
393 properties on the rigorous flux computations. Moreover, it is of crucial importance considering the
394 kinetic features of metal complexation when evaluating the toxicity through the organisms.
395 Currently, bioavailability and toxicity models are based only on the contribution of the free species,
396 however, due to the dynamic of these systems, consideration of the labile complex for the
397 internalization flux could be of great importance.

398

399 4.4 Toxicity evaluation

400 Despite the growing interest in the development of PFNCs, safety for human health and the
401 environment have not been properly addressed yet. The strict combination of polymers and NPs
402 (Ging et al., 2014) does not ease this investigation. NPs could pose some intrinsic potential risks.
403 For example, the biocompatibility investigations of graphene and graphene oxide have been
404 unsatisfactory with some papers demonstrating severe dose-dependent toxicity (Hu et al., 2011;
405 Wang et al., 2011), while others indicated that graphene NPs might improve cell growth (Lee et al.,
406 2011; Ruiz et al., 2011). Furthermore, not only the environmental toxicity, but also the fate of NPs
407 remains poorly understood, even for the most toxic NPs like Ag. As for toxicity effects, the fate of
408 NPs shows NP-specific partitioning behavior. Kaegi et al. (2013) evidenced little discharge for Ag
409 NPs into surface waters from urban wastewater cycle, whereas Ferry et al. (2009) demonstrated
410 how Au nano-rods could partition after an exposure period of 12 days in an aquatic mesocosm
411 being detectable in biofilm, the water column, clams and other biota. Preferably, the use of PFNCs
412 should reduce the release and potential toxic effects of NPs while the adsorption of the target
413 contaminant(s) by the nanocomposites should be comparable (or higher) than that obtained from the
414 free NPs (Önnby et al., 2014).

415 Currently, most data are referred mainly to PFNCs constituents and in just few cases to PFNC as a
416 whole. Tests on whole materials and after weathering experiments (e.g., UV ray, humidity, and
417 chemical and biological factors) are needed considering both *in vitro* and *in vivo* (eco)toxicology
418 (Posgai et al., 2011; Ging et al., 2014). Current research on the environmental stability of PFNCs
419 focused mostly on short-term stability, while the investigation of the long-term stability are missing.
420 Ging et al. (2014) investigated plain multi-walled carbon nanotubes (MWCNTs) and amino-
421 MWCNTs epoxy nanocomposites (after UV weathering for 1560 h) on *Drosophila melanogaster*
422 embryos (survivorship and developmental rate) showing no significant increase in toxicity,
423 probably because carbon nanotubes (CNTs) collected in abraded samples were still encapsulated in
424 the matrix, thus limiting the exposure. Paul et al. (2015) produced silver/polymer nanocomposites

425 functionalized by amino groups after reacting with end acidic groups from PLA and its co-polymer
426 with PLGA. While silver/polymer nanocomposites are used in biomedical materials and sensors
427 showing a low-toxicity for humans, but they inhibit the growth of a wide range of microorganisms
428 (Chaloupka et al., 2008). PLA (Jamshidian et al., 2010) and PLGA (Makadia et al., 2010) are well
429 known as non-toxic biodegradable materials (Danhier et al., 2012). PFNCs like silver/PLA and
430 silver/PLGA nanocomposites showed strong bactericidal properties (*Escherichia coli*) with almost
431 non-harmful effects to humans (Paul et al., 2015). Other PFNCs were mainly investigated for
432 biomedical applications (for orthopedic and dental applications) like injectable nanocomposites
433 made of biodegradable poly(-propylene fumarate) (Shi et al., 2008) proving the absence of
434 cytotoxicity (fibroblast cell line *in vitro* test).

435 Papers developing PFNC materials for specific water and wastewater applications did not
436 investigate any potential (eco)toxicity effects (Katsoyiannis and Zouboulis, 2002; Chang et al.,
437 2005; Guo and Chen, 2005; Chang et al., 2006; Say et al., 2006; Banerjee et al., 2007; Lim et al.,
438 2009; Wang and Wang, 2009; Zhou et al., 2009; Tran et al., 2010; Badruddoza, et al. 2011; Bée et
439 al., 2011; Shirsath et al., 2011; Zhu et al., 2011; Badruddoza et al., 2012; Badruddoza, et al.
440 2013a,b; Musico et al., 2013). An exception was done by Önnby et al. (2014), where they
441 investigated nanocomposites of aluminium oxide nanoparticles (Al NPs) incorporated in a PA
442 cryogel matrix for AsO_4^{3-} removal efficiency in the perspective of creating a water filter, also
443 demonstrating the potential toxicity of the filtrate by using human epithelial cells (Caco-2). No cell
444 death in relation to the presence of NP was evident, but cell viability was slightly affected probably
445 due to the levels of a residual monomer. Authors suggested further investigations stressing the
446 PNFC system performance using higher flow speeds and composite volumes, under more
447 aggressive pH conditions, and with higher ionic strength (Önnby et al., 2014).

448 Despite the use of PFNCs mainly as adsorbent for metals removal from water and wastewater,
449 several issues related to their safety are still open: i) in general few data on PFNC as a whole, and
450 very limited data for the specific water-related application is available; ii) existing stressing and

451 weathering experiments are occasional and short-term based; and iii) scarce toxicity data are
452 available only for cell lines and/or microorganisms still on a short time exposure, while no whole
453 multicellular eukaryotic biological models have been considered.

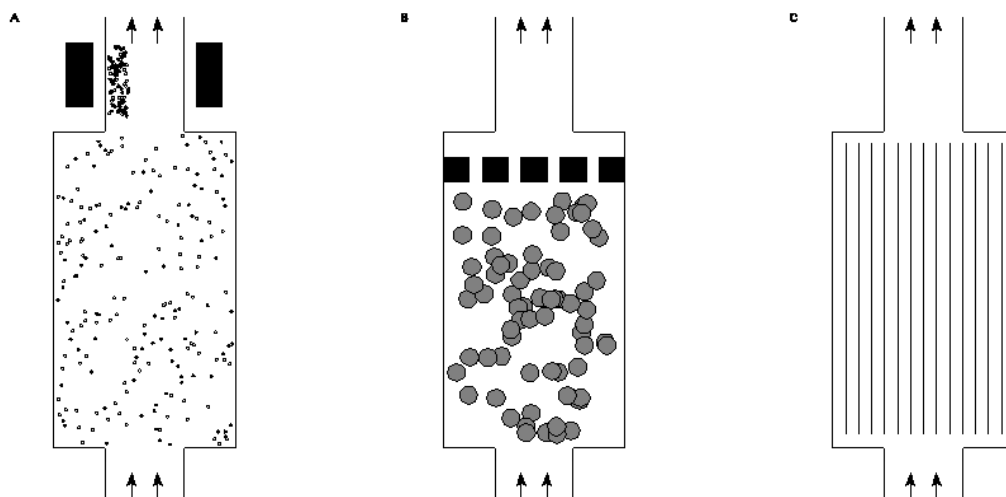
454

455 4.5 Design considerations

456 Most studies concerning metal removal via PFNCs are related to laboratory-scale set-ups. This
457 raises questions about the possibilities of deploying this technique into *in situ* situations. Lab-scale
458 configurations studies evidence three main configurations, as summarized in Figure 3:

- 459 • NPs are mixed with contaminated water, being the main problem of this approach the separation
460 of NPs from the water. However, if magnetic NPs are used, this can be achieved via magnetic
461 fields to overcome the main limitation of this approach (Manju et al., 2002).
- 462 • NPs are immobilized on membrane sheets or fibers and the contaminated water passes over
463 them making the adsorption process possible. The advantage of this design is that the NPs can
464 be recovered, but a suitable system (*i.e.* sufficient capacity) might require a large surface area
465 for efficient contaminants adsorption (Vatutsina et al., 2007). Membrane fouling is a current
466 problem requiring to regular cleaning procedure or membrane replacement.
- 467 • NPs can be immobilized onto larger particles that are easily separated from water at or near the
468 outlet of the treatment installation. This leads to a fixed bed or fluidized bed system, where the
469 water flows through the pores among the particles (Katsoyiannis and Zouboulis, 2002, Cumbal
470 and Sengupta, 2011). Fouling could reduce the effectiveness of the adsorption process, but the
471 replacement of larger particles can be continuous.
- 472 • NPs are immobilized on membrane sheets or fibers and the contaminated water passes over
473 them making adsorption possible. The advantage of this design is that the NPs can be recovered,
474 but a suitable system (*i.e.*, membrane fouling is a current problem requiring a regular cleaning
475 procedure or membrane replacement).

476



477

478 **Figure 3** Rough sketch of various designs: A) Free NPs which are separated from the water via a
 479 magnetic field; B) NPs immobilized on macroscopic particles (fixed or fluidized bed); C) NPs
 480 immobilized on membranes.

481

482 Crucial parameters for the design are i) the total surface area available for adsorption processes
 483 determining the capacity, and ii) the achievable throughput causing the system footprint. To better
 484 elucidate the scale effect we can consider a case study where Cd contaminates water. Table 3
 485 indicates an adsorption capacity of 21 mg Cd per g of PA-(HFO) (Manju et al., 2002), where the S-
 486 PFNCs are in suspension, so that the entire surface is available for adsorption. The total surface area
 487 per unit of volume ($\text{m}^2 \text{L}^{-1}$) is provided by Eq. 4.

$$488 \quad A = 4\pi R^2 N \quad (\text{Eq. 4})$$

489 where, R is the radius of the S-PFNCs (considering S-PFNCs as roughly spherical), and N is the
 490 number of NPs per unit of volume. This is related to the mass concentration C :

$$491 \quad N = C / (\rho \frac{4\pi}{3} R^3) \quad (\text{Eq. 5})$$

492 where, ρ is the density and the denominator is the mass per NP. Combining Eq. 4 and Eq. 5 leads to:

$$493 \quad A = 3C / \rho R \quad (\text{Eq. 6})$$

494 According to Eq. 6 and using a density of 4000 kg/m^3 and a radius of 50 nm , removal of 1 g/m^3 of
 495 these NPs corresponds to 5 m^2 surface area per m^3 of suspension.

496 Since this concerns free-floating NPs, the full surface area is available. If the NPs are embedded in
497 a polymer membrane, then roughly half of the surface will be available. Furthermore the NPs will
498 be spread over the membrane and they may or may not be close together. Assuming that the S-
499 PFNCs are indeed as close together as possible, then an estimate of the membrane area can be
500 obtained, which will in fact be a lower limit. The adsorption of 21 mg Cd requires 1 g of HFO.
501 From the above calculation the surface area of 1 g NPs is 5 m². Therefore at least 5 m² of membrane
502 are required to adsorb that amount of Cd and probably more, since the NPs will be spread over the
503 membrane rather than being very close together. This gives an idea of the dimensions of a device
504 intended to adsorb metals from water via such membranes.

505

506 **4.6 Cost evaluation**

507 The cost of the materials is one of the key factors to evaluate the sustainability of PFNCs as
508 adsorbents. The cost of producing PA - (HFO) is 7 US\$ per 100 g which is approximately three
509 times lower than the cost of some commercial resins such as Amberlite IRA-64, Amberlite IRP-88,
510 Amberlite CG-50 and Duolite ES-468 (21-45 US\$ per 100 g of resin) (Manju et al., 2002).

511 The cost of modification agents should also be estimated. For instance, α -KA is a harmless and
512 environmental-friendly biologic reagent, while chemical modification reagents are general toxic to
513 humans and animals, and also expensive. The cost of the α -KA- Ch - (γ -Fe₂O₃) is mainly related to
514 the α -KA price, which is about 380 US\$ per kg depending on the preparation procedure. However,
515 the costs of the chitosan flakes cross-linked with glutaraldehyde and chitosan-coated polyvinyl
516 chloride beads can reach up to 15,700 and 3,254 US\$ per kg, respectively. The removal efficiency
517 of α -KA- Ch - (γ -Fe₂O₃) reach 50% after 2 min, and its adsorption equilibrium can be attained after
518 60 min, whereas the equilibrium time for the chitosan flakes cross-linked with glutaraldehyde can
519 be 16 times faster. The maximum uptake of the α -KA- Ch - (γ -Fe₂O₃) is 96.15 mg g⁻¹, while that of
520 the chitosan flakes cross-linked with glutaraldehyde or chitosan-coated polyvinyl chloride beads is
521 85.5 or 87.9 mg g⁻¹, respectively. Therefore, the α -KA- Ch - (γ -Fe₂O₃) can be considered as a viable

522 economical alternative for the commercially available adsorbents for the removal of metals from
523 aqueous solutions (Zhou et al., 2009).

524

525 5. Conclusions

526 In the last decade, several studies have been devoted to the application of PFNCs for metals and
527 metalloids removal from water and wastewater. Despite the promises of these adsorbents, several
528 issues related to their use still remain to be addressed:

529 ▪ Safety for human health and the environment has not been fully assessed - further research
530 is expected in the near future investigating the long term exposure and effects considering
531 various biological targets;

532 ▪ Greening the PFNCs production is expected in order to minimize the use of solvents and
533 make their use more environmentally friendly;

534 ▪ Removal efficiency and cost optimization per unit volume treated waiting for an economy of
535 scale;

536 ▪ Support the life cycle impact analysis according to the reuse, recovery and regeneration
537 approaches and zero-waste perspective.

538

539 **Acknowledgments**

540 The authors thank COST – European Cooperation in Science and Technology – and the COST
541 Action ES1205 members for the kind support, exchange of ideas and discussions.

542

543 Nomenclature

α -KA = α -ketoglutaric acid

CA – (γ -Fe₂O₃) = Calcium alginate coated iron oxide

(C – β – CD) = Carboxymethyl- β -cyclodextrin

ACP – N(CH₃)₂ – (HFO) = Acrylic polymer +N(CH₃)₂ supported Hydrated Iron (III) Oxide

C – β – CD – (Fe₃O₄) = Carboxymethyl – β – cyclodextrin modified (Fe₃O₄)

CA – (Fe₃O₄) = Calcium alginate encapsulated (Fe₃O₄)

CA – (HFO) = Calcium alginate coated hydrous iron oxide

CDs = Cyclodextrins

Ce – (Fe₃O₄) = (Fe₃O₄)/bacterial cellulose

Ce – (HFO) = Cellulose loaded with hydrous iron oxide

Ch – (γ -Fe₂O₃) = Chitosan coated iron oxide

Ch – (Cu⁰) = Chitosan supported copper

Ch – (Fe₂O₃) = Chitosan supported iron oxide

CNTs = Carbon Nanotubes

CPDB – (HFO) = Polystyrene + Divinylbenzene copolymer coated by Hydrated Iron (III) Oxide

D001 – (HFO) = Hydrated Fe(III) oxide (HFO) Nanoparticles within a cation-exchange resin D-001

DETA – (Fe₃O₄) = Diethylenetriamine supported Fe₃O₄magnetic

EDA – (Fe₃O₄) = Ethylenediamine supported Fe₃O₄magnetic

FT – IR = Fourier Transform Infra-Red

GA – (Fe₃O₄) = Gum arabic supported (Fe₃O₄)

HFO = Hydrated Iron (III) Oxide

HSAB theory= Hard-Soft Acid-Base theory

MP – (Fe₃O₄) = Mercapto-functionalized core-shell nano-magnetic Fe₃O₄polymers

MWCNTs = Multi Walled Carbon Nanotubes

mPAA – (Fe₃O₄) = Magnetic polyacrylic acid sodium salt supported Fe₃O₄ magnetic

PA – (HFO) = Polyacrylamide grafted Hydrated Iron (III) Oxide

PA = Polyacrylamide

PA – (HFO) = Polyacrylamide-grafted hydrous iron(III) oxide

PEI – (Fe₃O₄) + SiO₂ = Polyethylenimine supported Fe₃O₄ magnetic

PEI – (Fe₃O₄) = Polyethylenimine supported Fe₃O₄ magnetic

PEI – C = Polyethylenimine supported nanocarbon

PEI – NC = Polyethylenimine nanocomposite

PLA = polylactide

PLCy – (γ-Fe₂O₃) = Poly-L-cysteine immobilized onto the surface of iron oxide

PLGA = polyglycolide

PnV – G = Poly (n- vinylcarbazole) blended with graphene oxide nanoparticles

PP = polypropylene

PS – (HFO) = Polystyrene sulfone supported Hydrated Iron (III) Oxide

PS – (HMO) = Polystyrene sulfone supported Hydrated Iron (III) Oxide

PS – ZrP = Polystyrene sulfone supported Zirconium phosphate

PS – Zr(HPO₃S)₂ = Polystyrene sulfone supported Zirconium hydrogen monothio phosphate

SEM = Scanning Electron Microscopy

SPM = Scanning Probe Microscopy

TEM = Transmission Electron Microscopy

TEPA – (Fe₃O₄) = Tetraethylenepentamine supported Fe₃O₄ magnetic

TETA – (Fe₃O₄) = Triethylenetetramine supported Fe₃O₄ magnetic

XRD = X-Ray Diffraction

546 6. References

- 547 Badruddoza, A.Z.M., Tay, A.S.H., Tan, P.Y., Hidajat, K., and Uddin, M.S. (2011). Carboxymethyl-
548 β -cyclodextrin conjugated magnetic nanoparticles as nano-adsorbents for removal of copper ions:
549 Synthesis and adsorption studies. *J. Hazard. Mater.* 185, 1177–1186.
- 550 Badruddoza, A.Z.M., Shawon, Z.B.Z., Tay, W.J.D., Hidajat, K., and Uddin, M.S. (2012).
551 Fe₃O₄/cyclodextrin polymer nanocomposites for selective heavy metals removal from industrial
552 wastewater. *Carbohydr. Polym.* 91, 322–332.
- 553 Badruddoza, A.Z.M., Shawon, Z.B.Z., Tay, D.W.J., Hidajat, K., and Uddin, M.S. (2013). Endocrine
554 Disrupters and Toxic Metal Ions Removal by Carboxymethyl- β -Cyclodextrin Polymer Grafted onto
555 Magnetic Nanoadsorbents. *J. Chem. Eng.* 27.
- 556 Banerjee, S.S., and Chen, D.-H. (2007). Fast removal of copper ions by gum arabic modified
557 magnetic nano-adsorbent. *J. Hazard. Mater.* 147, 792–799.
- 558 Bée, A., Talbot, D., Abramson, S., and Dupuis, V. (2011). Magnetic alginate beads for Pb(II) ions
559 removal from wastewater. *J. Colloid Interface Sci.* 362, 486–492.
- 560 Bibak, A. (1994). Cobalt, copper, and manganese adsorption by aluminium and iron oxides and
561 humic acid. *Commun. Soil Sci. Plant Anal.* 25, 3229–3239.
- 562 Carotenuto M., Lofrano G., Siciliano A., Aliberti F., Guida M. (2014) TiO₂ photocatalytic
563 degradation of caffeine and ecotoxicological assessment of oxidation by-products. *Global Nest*
564 *Journal* 16 (3), 265-275.
- 565 Chaloupka K., Malam Y., Seifalian A.M., Nanosilver as a new generation of nanoparticle in
566 biomedical applications, *Trends Biotechnol.* 28 (2010)580–588.

567 Chang, Y.-C., and Chen, D.-H. (2005). Preparation and adsorption properties of monodisperse
568 chitosan-bound Fe₃O₄ magnetic nanoparticles for removal of Cu(II) ions. *J. Colloid Interface Sci.*
569 283, 446–451.

570 Crini, G., and Peindy, H.N. (2006). Adsorption of C.I. Basic Blue 9 on cyclodextrin-based material
571 containing carboxylic groups. *Dyes Pigments* 70, 204–211.

572 Cumbal, L., and Sengupta, A.K. (2005). Arsenic removal using polymer-supported hydrated
573 iron(III) oxide nanoparticles: role of donnan membrane effect. *Environ. Sci. Technol.* 39, 6508–
574 6515.

575 Danhier F., Ansorena E., Silva J.M., Coco R., Le Breton A., Pr at V., PLGA-based nanoparticles:
576 an overview of biomedical applications, *J. Control. Release* 161(2012) 505–522.

577 Davis, A.P., and Bhatnagar, V. (1995). Adsorption of cadmium and humic acid onto hematite.
578 *Chemosphere* 30, 243–256.

579 De Marco, M.J., SenGupta, A.K., and Greenleaf, J.E. (2003). Arsenic removal using a
580 polymeric/inorganic hybrid sorbent. *Water Res.* 37, 164–176.

581 Domingos Rute F, G elabert Alexandre, Carreira Sara, Cordeiro Ana, Sivry Yann, Benedetti Marc F.
582 Metals in the aquatic environment – interactions and implications for the speciation and
583 bioavailability: a critical overview. *Aquatic Geochemistry* (2015) 21, 231-257. DOI:
584 10.1007/s10498-014-9251-x

585 Ferry JL, Craig P, Hexel C, Sisco P, Frey R, Pennington PL, et al. Transfer of gold nanoparticles
586 from the water column to the estuarine food web. *Nat Nanotechnol* 2009;4: 441–4.

587 Freundlich, H. (1906).  ber die Adsorption in L sungen (Wilhelm Engelmann).

588 Ghorbani, M., and Eisazadeh, H. (2013). Removal of COD, color, anions and heavy metals from
589 cotton textile wastewater by using polyaniline and polypyrrole nanocomposites coated on rice husk
590 ash. *Compos. Part B Eng.* 45, 1–7.

591 Ging, J., Tejerina-Anton, R., Ramakrishnan, G., Nielsen, M., Murphy, K., Gorham, J.M., Nguyen,
592 T. and Orlov, A. (2014) Development of a conceptual framework for evaluation of nanomaterials
593 release from nanocomposites: Environmental and toxicological implications. *Science of The Total*
594 *Environment* 473-474, 9-19.

595 Grassi M., Kaykioglu G., Belgiorno V. and Lofrano G. (2012) Removal of Emerging Contaminants
596 from Water and Wastewater by Adsorption Process. In *Emerging compounds removal from*
597 *wastewater. Natural and solar based treatments* (G. Lofrano, Ed) Springer ISBN 978-9-4007-3915-
598 4

599 Guo, X., and Chen, F. (2005). Removal of Arsenic by Bead Cellulose Loaded with Iron
600 Oxyhydroxide from Groundwater. *Environ. Sci. Technol.* 39, 6808–6818.

601 Herman P. van Leeuwen. Revisited the conception of lability of metal complexes. *Electroanalysis*
602 (2001) 13, 826–830.doi:10.1002/1521-4109(200106)13:10\826:AID-ELAN826[3.0.CO;2-J

603 Hu W., C. Peng, M. Lv, X. Li, Y. Zhang, N. Chen, C. Fan and Q. Huang, *ACS Nano*, 2011, 5,
604 3693–3700.

605 Jamshidian M., Tehrany E.A., Imran M., Jacquot M., Desobry S., Poly-lactic acid:production,
606 applications, nanocomposites, and release studies, *Compre. Rev.Food Sci. Food Saf.* 9 (2010) 552–
607 571.

608 Jin J., Li R., Wang H.L., Chen H.N., Liang K., Ma J.T., Magnetic Fe nanoparticle functionalized
609 water-soluble multi-walled carbon nanotubules towards the preparation of sorbent for aromatic
610 compounds removal, *Chem. Commun.* 4 (2007) 386–388.

611 Kaegi R, Voegelin A, Ort C, Sinnet B, Thalmann B, Krismer J, et al. Fate and transformation of
612 silver nanoparticles in urban wastewater systems. *Wat. Res.* 2013;47(12):3866–77.

613 Katsoyiannis, I.A., and Zouboulis, A.I. (2002). Removal of arsenic from contaminated water
614 sources by sorption onto iron-oxide-coated polymeric materials. *Water Res.* 36, 5141–5155.

615 Khaydarov, R.A., Khaydarov, R.R., and Gapurova, O. (2010). Water purification from metal ions
616 using carbon nanoparticle-conjugated polymer nanocomposites. *Water Res.* 44, 1927–1933.

617 Khare H.S. and Burris D.L., A quantitative method for measuring nanocomposite dispersion,
618 *Polymer* 51 (2010) 719–729

619 Langmuir, I. (1918). THE ADSORPTION OF GASES ON PLANE SURFACES OF GLASS,
620 MICA AND PLATINUM. *J. Am. Chem. Soc.* 40, 1361–1403.

621 Lee W. C., C. H. Y. X. Lim, H. Shi, L. A. L. Tang, Y. Wang, C. T. Lim and K. P. Loh, *ACS Nano*,
622 2011, 5, 7334–7341.

623 Lim, S.-F., Zheng, Y.-M., Zou, S.-W., and Chen, J.P. (2009). Removal of copper by calcium
624 alginate encapsulated magnetic sorbent. *Chem. Eng. J.* 152, 509–513.

625 Mahdavian, A.R., and Mirrahimi, M.A.-S. (2010). Efficient separation of heavy metal cations by
626 anchoring polyacrylic acid on superparamagnetic magnetite nanoparticles through surface
627 modification. *Chem. Eng. J.* 159, 264–271.

628 Makadia H.K., Siegel S.J., Poly lactic-co-glycolic acid (PLGA) as biodegradable controlled drug
629 delivery carrier, *Polymers* 3 (2011) 1377–1397.

630 Manju, G.N., Anoop Krishnan, K., Vinod, V.P., and Anirudhan, T.S. (2002). An investigation into
631 the sorption of heavy metals from wastewaters by polyacrylamide-grafted iron(III) oxide. *J. Hazard.*
632 *Mater.* 91, 221–238.

633 Michler, G.H. (Ed.), *Electron Microscopy of in Polymers*, Springer Verlag: Heidelberg, 2008

634 Millon, L.E., and Wan, W.K. (2006). The polyvinyl alcohol–bacterial cellulose system as a new
635 nanocomposite for biomedical applications. *J. Biomed. Mater. Res. B Appl. Biomater.* 79B, 245–
636 253.

637 Möller T., Sylvester P. (2008) Effect of silica and pH on arsenic uptake by resin/iron oxide hybrid
638 media. *Water Res.* 442, 1760 – 1766

639 Nah I.W., Hwang K.Y., Jeon C., Choi H.B., Removal of Pb ion from water by magnetically
640 modified zeolite, *Miner. Eng.* 19 (2006) 1452–1455.

641 Nassar, N. N. (2010). Rapid removal and recovery of Pb(II) from wastewater by magnetic
642 nanoadsorbents. *Journal of Hazardous Materials*, 184, 538– 546.

643

644 Nishikawa, M., Ishibashi, H., and Furukawa, H. (1984). Process for preparing porous spherical
645 cellulose particles.

646 Norkus, E. (2009). Metal ion complexes with native cyclodextrins. An overview. *J. Incl. Phenom.*
647 *Macrocycl. Chem.* 65, 237–248.

648 Önnby, L., Svensson, C., Mbundi, L., Busquets, R., Cundy, A., & Kirsebom, H. (2014). γ -Al₂O₃-
649 based nanocomposite adsorbents for arsenic (V) removal: Assessing performance, toxicity and
650 particle leakage. *Science of the Total Environment*, 473, 207-214.

651 Pan, B., Pan, B., Chen, X., Zhang, W., Zhang, X., Zhang, Q., Zhang, Q., and Chen, J. (2006).
652 Preparation and preliminary assessment of polymer-supported zirconium phosphate for selective
653 lead removal from contaminated water. *Water Res.* 40, 2938–2946.

654 Pan, B., Su, Q., Zhang, W., Zhang, Q., Ren, H., Zhang, Q. et al., (2007). A process to prepare a
655 hybrid sorbent by impregnating hydrous manganese dioxide (HMO) nanoparticles within polymer
656 for enhanced removal of heavy metals. Chinese Patent No.. ZL 200710134050.9.

657 Pan, B., Pan, B., Zhang, W., Lv, L., Zhang, Q., and Zheng, S. (2009). Development of polymeric
658 and polymer-based hybrid adsorbents for pollutants removal from waters. *Chem. Eng. J.* *151*, 19–
659 29.

660 Pan, B., Qiu, H., Pan, B., Nie, G., Xiao, L., Lv, L., Zhang, W., Zhang, Q., and Zheng, S. (2010).
661 Highly efficient removal of heavy metals by polymer-supported nanosized hydrated Fe(III) oxides:
662 Behavior and XPS study. *Water Res.* *44*, 815–824.

663 Pan, S., Zhang, Y., Shen, H., and Hu, M. (2012). An intensive study on the magnetic effect of
664 mercapto-functionalized nano-magnetic Fe₃O₄ polymers and their adsorption mechanism for the
665 removal of Hg(II) from aqueous solution. *Chem. Eng. J.* *210*, 564–574.

666 Pang, Y., Zeng, G., Tang, L., Zhang, Y., Liu, Y., Lei, X., Li, Z., Zhang, J., and Xie, G. (2011a).
667 PEI-grafted magnetic porous powder for highly effective adsorption of heavy metal ions.
668 *Desalination* *281*, 278–284.

669 Pang, Y., Zeng, G., Tang, L., Zhang, Y., Liu, Y., Lei, X., Li, Z., Zhang, J., Liu, Z., and Xiong, Y.
670 (2011b). Preparation and application of stability enhanced magnetic nanoparticles for rapid removal
671 of Cr(VI). *Chem. Eng. J.* *175*, 222–227.

672 Paul, A., Kaverina, E., Vasiliev, A., 2015. Synthesis of silver/polymer nanocomposites by surface
673 coating using carbodiimide method. *Colloids and Surfaces A: Physicochemical and Engineering*
674 *Aspects* *482*, 44-49.

675 Posgai R, Cipolla-McCulloch CB, Murphy KR, Hussain SM, Rowe JJ, Nielsen MG. Differential
676 toxicity of silver and titanium dioxide nanoparticles on *Drosophila melanogaster* development,

677 reproductive effort, and viability: Size, coatings and antioxidants matter. *Chemosphere*
678 2011;85(1):34–42.

679 Ruiz O. N., K. A. S. Fernando, B. Wang, N. A. Brown, P. G. Luo, N. D. McNamara, M. Vangsness,
680 Y.-P. Sun and C. E. Bunker, *ACS Nano*, 2011, 5, 8100–8107.

681 Qu, X., Alvarez, P.J.J., and Li, Q. (2013). Applications of nanotechnology in water and wastewater
682 treatment. *Water Res.* 47, 3931–3946.

683 Sarkar, S., Chatterjee, P.K., Cumbal, L.H., and SenGupta, A.K. (2011). Hybrid ion exchanger
684 supported nanocomposites: Sorption and sensing for environmental applications. *Chem. Eng. J.*
685 166, 923–931.

686 Shen, Haoyu, et al. "A new insight on the adsorption mechanism of amino-functionalized nano-Fe₃
687 O₄ magnetic polymers in Cu (II), Cr (VI) co-existing water system." *Chemical Engineering*
688 *Journal* 183 (2012): 180-191.

689 Shi, X., Sitharaman, B., Pham, Q.P., Spicer, P.P., Hudson, J.L., Wilson, L.J., Tour, J.M., Raphael,
690 R.M., Mikos, A.G., 2008. In vitro cytotoxicity of single-walled carbon nanotube/biodegradable
691 polymer nanocomposites. *Journal of Biomedical Materials Research Part A* 86A, 813-823.

692 Sylvester, P., Westerhoff, P., Möller, T., Badruzzaman, M., and Boyd, O. (2007). A Hybrid Sorbent
693 Utilizing Nanoparticles of Hydrous Iron Oxide for Arsenic Removal from Drinking Water. *Environ.*
694 *Eng. Sci.* 24, 104–112.

695 Szejtli, J. (1998). Introduction and General Overview of Cyclodextrin Chemistry. *Chem. Rev.* 98,
696 1743–1754.

697 Tran, H.V., Tran, L.D., and Nguyen, T.N. (2010). Preparation of chitosan/magnetite composite
698 beads and their application for removal of Pb(II) and Ni(II) from aqueous solution. *Mater. Sci. Eng.*
699 *C 30*, 304–310.

700 Vatutsina, O.M., Soldatov, V.S., Sokolova, V.I., Johann, J., Bissen, M., and Weissenbacher, A.
701 (2007). A new hybrid (polymer/inorganic) fibrous sorbent for arsenic removal from drinking water.
702 *React. Funct. Polym.* *67*, 184–201.

703 Wang, J., Gerlach, J.D., Savage, N., and Cobb, G.P. (2013). Necessity and approach to integrated
704 nanomaterial legislation and governance. *Sci. Total Environ.* *442*, 56–62.

705 Wang K., J. Ruan, H. Song, J. Zhang, Y. Wo, S. Guo and D. Cui, *Nanoscale Res. Lett.*, 2011, 6, 1–
706 8.

707 Weber, T.W., and Chakravorti, R.K. (1974). Pore and solid diffusion models for fixed-bed
708 adsorbers. *AIChE J.* *20*, 228–238.

709 White, B. R., Stackhouse, B. T., Holcombe, J. A (2009) Magnetic γ -Fe₂O₃ nanoparticles coated
710 with poly-L-cysteine for chelation of As(III), Cu(II), Cd(II), Ni(II), Pb(II) and Zn(II). *J.Haz Mat.*
711 *161*, 848–853

712

713 Wu, S.-J., Liou, T.-H., and Mi, F.-L. (2009). Synthesis of zero-valent copper-chitosan
714 nanocomposites and their application for treatment of hexavalent chromium. *Bioresour. Technol.*
715 *100*, 4348–4353.

716 Xu S.H., Shangguan W., Yuan J., Chen M.X., Shi J.W., *Appl. Catal. B* *71* (2007)

717 Yu, L., Zou, R., Zhang, Z., Song, G., Chen, Z., Yang, J., et al. (2011). A Zn₂GeO₄-
718 ethylenediamine hybrid nanoribbon membrane as a recyclable adsorbent for the highly efficient
719 removal of heavy metals from contaminated water. *Chemical Communications*, 47, 10719–10721.
720

721 Zhang, Q., Pan, B., Pan, B., Zhang, W., Jia, K., and Zhang, Q. (2008). Selective sorption of lead,
722 cadmium and zinc ions by a polymeric cation exchanger containing nano-Zr(HPO₃S)₂. *Environ.*
723 *Sci. Technol.* 42, 4140–4145.

724 Zhao, X., Lv, L., Pan, B., Zhang, W., Zhang, S., and Zhang, Q. (2011). Polymer-supported
725 nanocomposites for environmental application: A review. *Chem. Eng. J.* 170, 381–394.

726 Zhao, Y.-G., Shen, H.-Y., Pan, S.-D., Hu, M.-Q., and Xia, Q.-H. (2010). Preparation and
727 characterization of amino-functionalized nano-Fe₃O₄ magnetic polymer adsorbents for removal of
728 chromium(VI) ions. *J. Mater. Sci.* 45, 5291–5301.

729 Zhou, Y.-T., Nie, H.-L., Branford-White, C., He, Z.-Y., and Zhu, L.-M. (2009). Removal of Cu²⁺
730 from aqueous solution by chitosan-coated magnetic nanoparticles modified with alpha-ketoglutaric
731 acid. *J. Colloid Interface Sci.* 330, 29–37.

732 Zhu, H., Jia, S., Wan, T., Jia, Y., Yang, H., Li, J., Yan, L., and Zhong, C. (2011). Biosynthesis of
733 spherical Fe₃O₄/bacterial cellulose nanocomposites as adsorbents for heavy metal ions. *Carbohydr.*
734 *Polym.* 86, 1558–1564.

735 Zouboulis A. I. and Katsoyiannis I. A. (2002) Arsenic Removal Using Iron Oxide Loaded Alginate
736 Beads *Ind. Eng. Chem. Res.* 41, 6149-6155
737
738

739

740 Figures Captions

741 **Figure 1** Fabrication methods of PFNCs

742 **Figure 2** Schematic representations of the polymeric cation and anion exchangers used on the S-
743 PFNCs HFO - Hydrated iron (III) oxide. (Modified from Cumbal and Sengupta, 2005

744 **Figure 3** Rough sketch of various designs: A. Free NPs which are separated from the water via a
745 magnetic field; B. NPs immobilized on macroscopic particles (fixed or fluidized bed); C. NPs
746 immobilized on membranes.

747

748

749

750 Table Captions

751 **Table 1** Synthesis of Synthetic polymer functionalized nanocomposites (S- PFNCs)

752 **Table 2** Synthesis of Biopolymers functionalized nanocomposites (B- PFNCs)

753 **Table 3** Behaviour of S- PFNCs for metal removal

754 **Table 2** Behaviour of S B- PFNCs- adsorption

755

756

757

758

Table 1

<i>Polymer matrix</i>	NPs	S-PFNCs	Preparation method	Ref.
<i>Polystyrene sulfone</i>	Hydrated iron oxide (HFO)	PS-(HFO)	<i>In situ</i> synthesis ¹	Etzel et al., 1997
	Hydrated iron oxide (HFO)	PS-(HFO)	<i>In situ</i> synthesis ¹	Cumbal and Sengupta., 2005
	Hydrated iron oxide (HFO)	PS-(HFO)	<i>In situ</i> synthesis ¹	DeMarco et al., 2002
	Hydrated iron oxide (HFO)	PS-(HFO)	<i>In situ</i> synthesis ¹	Sylvester et al., 2007
	Hydrated iron oxide (HFO)	PS-(HFO)	<i>In situ</i> synthesis ¹	Möller et al., 2008
	Hydrated iron oxide (HFO)	PS-(HFO)	<i>In situ</i> synthesis ¹	Pan et al., 2010
	Hydrous manganese oxide (HMO)	PS-(HMO)	<i>In situ</i> synthesis ¹	Pan et al., 2007
	Zirconium hydrogen monothio phosphate $Zr(HPO_3S)_2$	PS- $Zr(HPO_3S)_2$	<i>In situ</i> synthesis ¹	Zhang et al., 2008
	Zirconium phosphate	PS-ZrP	<i>In situ</i> synthesis ¹	Pan et al., 2006
<i>Copolymer (Polystyrene+divi</i>	Hydrated iron oxide	CPDB- (HFO)	Direct compounding	Katsoyiannis et al, 2002

<i>nylbenzene)</i>	(HFO)			
<i>Acrylic polymer +N(CH₃)₂</i>	Hydrated iron oxide (HFO)	ACP- N(CH ₃) ₂ - (HFO)	<i>In situ</i> synthesis ¹	Vatutsina et al., 2007
<i>Polyacrylamide</i>	Hydrated iron oxide (HFO)	PA-(HFO)	<i>In situ</i> synthesis ²	Manju et al, 2002
<i>Mercapto – functionalized polymer</i>	Magnetite (Fe ₃ O ₄)	MP- (Fe ₃ O ₄)	<i>In situ</i> synthesis ¹	Pan et al, 2012
<i>Polyethylenimine</i>	Magnetite (Fe ₃ O ₄)	PEI-(Fe ₃ O ₄)	Direct compounding	Pang et al, 2011b
	Magnetite (Fe ₃ O ₄) +SiO ₂	PEI-(Fe ₃ O ₄) +SiO ₂	Direct compounding	Pang et al, 2011a
	C	PEI-C	<i>In situ</i> synthesis ¹	Khaydarov et al, 2010
<i>m-PAA-Na</i>	Magnetite (Fe ₃ O ₄)	m-PAA – Na- (Fe ₃ O ₄)	<i>In situ</i> synthesis ²	Mahdavian et al, 2010
<i>Ammino-functionalized polymer (TEPA)</i>	Magnetite (Fe ₃ O ₄)	TEPA- (Fe ₃ O ₄)	<i>In situ</i> synthesis ²	Zhao et al., 2010
	Magnetite (Fe ₃ O ₄)	TEPA- (Fe ₃ O ₄)	<i>In situ</i> synthesis ²	Shen et al., 2012
<i>Poly (n-vinylcarbazole)</i>	Graphene oxide	PnV- G	Direct compounding	Musico et al., 2013

^{1,2} These numbers are referred to the preparation methods shown in Figure 1

Table 2

Polymer matrix	NPs	B-PNCs	Preparation method	Ref.
Calcium alginate	Iron oxide (Fe ₂ O ₃)	CA-(γ -Fe ₂ O ₃)	In <i>situ</i> synthesis ²	Bèe et al, 2011
	Hydrated iron oxide (HFO)	CA-(HFO)	Direct compounding	Zouboulis et al., 2002
	Magnetite (Fe ₃ O ₄)	CA-(Fe ₃ O ₄)	-	Lim et al., 2009
Carboxymethyl – β – cyclodextrin	Magnetite (Fe ₃ O ₄)	C- β -CD- (Fe ₃ O ₄)	In <i>situ</i> synthesis ²	Badruddoza et al., 2011, 2012, 2013
		C- β -CD- (Fe ₃ O ₄)	-	Yu et al. 2011
Cellulose	Hydrated iron oxide (HFO)	Ce - (HFO)	In <i>situ</i> synthesis ²	Guoand Chen 2005
	Magnetite (Fe ₃ O ₄)	Ce - (Fe ₃ O ₄)	In <i>situ</i> synthesis ²	Zhu et al., 2011
Chitosan	Iron oxide (Fe ₂ O ₃)	Ch - (γ -Fe ₂ O ₃)	In <i>situ</i> synthesis ²	Zhou et al., 2009
	Magnetite (Fe ₃ O ₄)	Ch-(Fe ₃ O ₄)	In <i>situ</i> synthesis ²	Tran et al., 2010
	Magnetite (Fe ₃ O ₄)	Ch-(Fe ₃ O ₄)	In <i>situ</i> synthesis ²	Chang and Chen, 2005
	Magnetite (Fe ₃ O ₄)	Ch-(Fe ₃ O ₄)	In <i>situ</i> synthesis ²	Chang et al, 2006
	Cu ⁰	Ch-(Cu ⁰)	In <i>situ</i> synthesis ²	Wu et al, 2009
Gum arabic	Magnetite (Fe ₃ O ₄)	GA-(Fe ₃ O ₄)	In <i>situ</i> synthesis ²	Banerjee and Chen, 2007
Poly-L-cysteine	Iron oxide (Fe ₂ O ₃)	PLCy-(γ -Fe ₂ O ₃)	In <i>situ</i> synthesis ²	White et al., 2009

²The number is referred to the preparation methods shown in Figure 1

Table 3

Metals	S-PFNPs	pH	C _o [mg L ⁻¹]	Adsorption capacities	Removal (%)	Adsorption constants	References
As(III)	PS – (HFO)	7.2	0.100	< 10 ppb within 2000 BV	> 90		De Marco et al., 2002
	PS – (HFO)		100	< 10 ppb within 12 000 BV	> 90	-	Cumbal and Sengupta, 2005
	ACP – N(CH ₃) ₂ – (HFO)	9	60	< 10 ppb within 10000 BV	90	K _L = 1.52 L mmol ⁻¹ K _F = 0.58 L mmol ⁻¹	Vatutsina et al., 2007
As(V)	PS – (HFO)		100	< 0.5 ppm	> 95	-	Etzel et al., 1997
	PS – (HFO)	7.2	0.050	< 10 ppb within 4000 BV	> 80		De Marco et al., 2002
	PS – (HFO)		0.100	< 10 ppb within 10 000 BV,	> 90	-	Cumbal and Sengupta, 2005
	PS – (HFO)	8.16	0.023	< 0.5 ppb within 33196 BV	> 98		Sylvester et al., 2007
	PS – (HFO)		0.020	< 10 ppb within 17500 BV	> 50		Möller et al., 2008
			0.300	< 10 ppb within 3500 BV	> 96		
	CPDB – (HFO)		0.100	< 10 ppb within 65 BV	90		Katsoyiannis and Zouboulis, 2002
ACP – N(CH ₃) ₂ – (HFO)	5.64	60	< 10 ppb within 10000 BV	90	K _L = 3.23 L mmol ⁻¹ K _F = 0.68 L mmol ⁻¹	Vatutsina et al., 2007	
Cd(II)	PA – (HFO)	5 - 6	25	21.03 mg g ⁻¹	81	K _L = 0.0206L mg ⁻¹	Manju et al, 2002

	PS – (HFO)		1	< 5 ppb within 7000 BV	> 99		Pan et al., 2007
	PS – HMO			sorption capacities increased by 50 – 300% compared to host exchangers		K_d increased by 20 – 800 times as compared to host exchangers	Pan et al., 2008
	PS – Zr(HPO ₃ S)		45	< 0.09 mg L ⁻¹ within 1600 BV	> 99	-	Zhang et al., 2008
	m-PAA – Na – (Fe ₃ O ₄)	8	1.8	5.0 mg g ⁻¹	-		Mahdavian et al, 2010
	PEI – C	6	3	< 0.005 ppm	99	-	Khaydarov et al, 2010
	PEI – (Fe ₃ O ₄) + SiO ₂	6.5	100	105.2 mg g ⁻¹	78	$K_L = 0.0290 \text{ L mg}^{-1}$ $K_F = 11.545 \text{ L g}^{-1}$	Pang et al, 2011a
Cr (VI)	PEI – (Fe ₃ O ₄)	2 – 3		83.33 mg g ⁻¹	95	$K_L = 0.125 \text{ L mg}^{-1}$ $K_F = 20.85 \text{ L g}^{-1}$	Pang et al, 2011b
	TEPA – (Fe ₃ O ₄)			370.37 mg g ⁻¹		$K_L = 0.1233 \text{ L mg}^{-1}$	Zhao et al., 2010
	TEPA – (Fe ₃ O ₄)	2	50 500 1000		99 73 42		Shen et al., 2012
Cu (II)	PS – (HFO)		1	< 5 ppb within 7000 BV	> 99	-	Pan et al., 2007
	PEI – (Fe ₃ O ₄) + SiO ₂	6.5	100	157.8 mg g ⁻¹	98	$K_L = 0.0318 \text{ L mg}^{-1}$ $K_F = 42.561 \text{ L g}^{-1}$	Pang et al, 2011a
	PEI – C	6	10	< 0.005 ppm	99		Khaydarov et al, 2010
	m-PAA – Na – (Fe ₃ O ₄)	8	18	27.0 mg g ⁻¹	-	-	Mahdavian et al, 2010

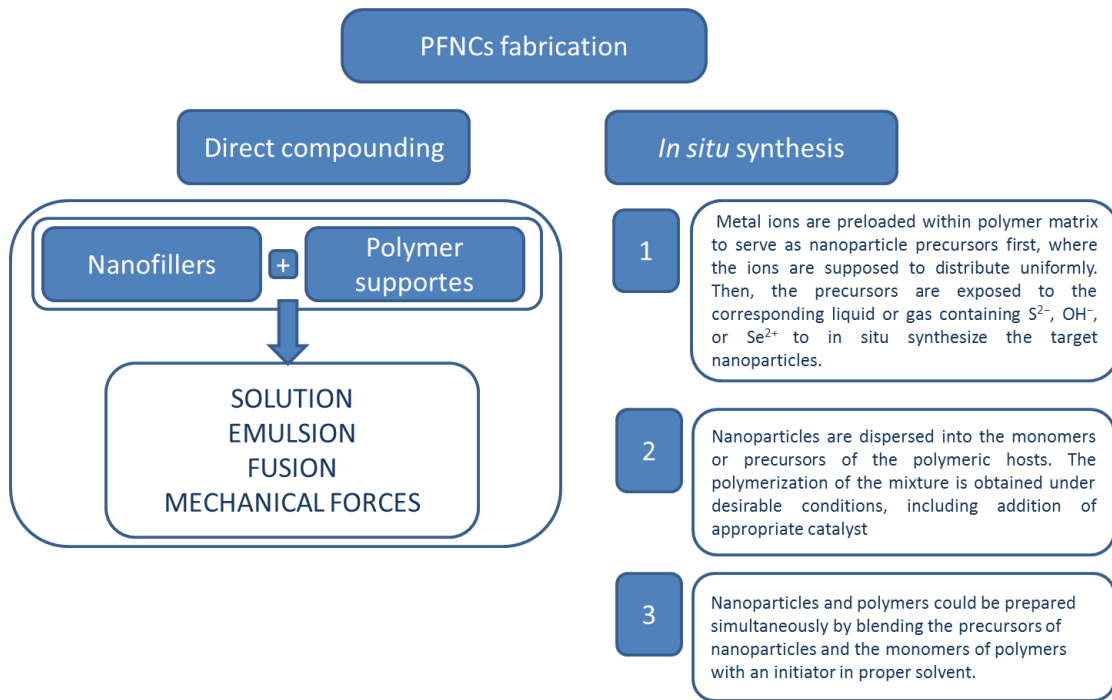
	TEPA – (Fe ₃ O ₄)	4	10 100 300	116.80 mg g ⁻¹	99.85 78.51 17.66	K _L = 0.4009 L mg ⁻¹	Shen et al., 2012
Hg(II)	PA – (HFO)	5	25	21.38 mg g ⁻¹	85	K _L = 0.0246 L mg ⁻¹	Manju et al, 2002
	MP – (Fe ₃ O ₄)	2 - 6	-	256.4 mg g ⁻¹	-	K _L = 0.0585 L mg ⁻¹ K _F = 50.54 L g ⁻¹	Pan et al, 2012
Ni(II)	m-PAA – Na – (Fe ₃ O ₄)		18	25.0 mg g ⁻¹	-	-	Mahdavian et al, 2010
Pb(II)	PS – HMO			sorption capacities increased by 50 – 300% compared to host exchangers		K _d increased by 20 – 800 times as compared to host exchangers	Pan et al., 2008
	PA – (HFO)	6	25	23.79 mg g ⁻¹	96	K _L = 0.0250 L mg ⁻¹	Manju et al, 2002
	PS – Zr(HPO ₃ S)		80	< 0.01 mg L ⁻¹ within 1600 BV	> 99	-	Zhang et al., 2008
	PS – ZrP		0.5	< 0.05 ppm within 2000 BV	98		Pan et al., 2006
	PS – (HFO)		1	< 5 ppb within 7000 BV	> 99		Pan et al., 2010
	m-PAA – Na – (Fe ₃ O ₄)	8	18	40.0 mg g ⁻¹	-		Mahdavian et al, 2010
	PnV – G	7	5 – 300	982.86 mg g ⁻¹	97	K _L = 0.0187 L mg ⁻¹	Musico et al., 2013
Zn(II)	PS – HMO			sorption capacities increased by 50 – 300% compared to host exchangers		K _d increased by 20 – 800 times as compared to host exchangers	Pan et al., 2007
	PS – Zr(HPO ₃ S) ₂		15	< 0.06 mg L ⁻¹ within	> 99		Zhang et al., 2008

				120 BV			
	PEI – C	6	5	< 0.010 ppm	99		Khaydarov et al, 2010
	PEI – (Fe ₃ O ₄) + SiO ₂	6.5	100	138.8 mg g ⁻¹	80%	K _L = 0.0245 L mg ⁻¹ K _F = 33.986 L g ⁻¹	Pang et al, 2011a
Se(IV)	PS – (HFO)		100	< 0.5 ppm	> 99	-	Etzel et al., 1997

Table 4

Metals	B-PFNCs	Optimum pH	C _o [mg L ⁻¹]	Adsorption capacities	Removal (%)	Adsorption constants K _L [L mg ⁻¹] K _F [L g ⁻¹]	References
As(III)	CA- (HFO)	7	0.05	< 10 ppb within 45 BV	> 95	-	Zouboulis and Katsoyiannis, 2002
	Ce - (HFO)	7 – 9	7.5	99.6 mg g ⁻¹	95	K _L = 0.120	Guo and Chen, 2005
	PLCy – (γ-Fe ₂ O ₃)	7 (4 – 9)	1	25.6 mg g ⁻¹	22	-	White et al., 2009
As(V)	CA- (HFO)	7	0.05	< 10 ppb within 230 BV	> 95	-	Zouboulis and Katsoyiannis, 2002
	Ce - (HFO)	7 (5 – 11)	7.5	33.2 mg g ⁻¹	90	K _L = 2.29	Guo and Chen, 2005
Au (III)	Ch- (Fe ₃ O ₄)	2 (2 – 10)	1039 (200 – 3000)	59.52 mg g ⁻¹		K _L = 0.066 K _F = 13.14	Chang and Chen, 2006
Cu (II)	CA- (Fe ₃ O ₄)	5 (2 – 6)	1 (1 – 6)	60 mg g ⁻¹		K _L = 1.43	Lim et al., 2009
	C-β- CD- (Fe ₃ O ₄)	6 (2 – 6)	(50 – 200)	47.2 mg g ⁻¹		K _L = 0.0237 K _F = 7.064	Badruddoza et al., 2011
	Ch - (γ-Fe ₂ O ₃)	6 (2 – 8)	200 (100 – 400)	96.15 mg g ⁻¹	55 – 99	K _L = 0.0493 K _F = 16.406	Zhou et al., 2009
	Ch- (Fe ₃ O ₄)	5 (2 – 5)	1150 (200 – 1150)	21.5 mg g ⁻¹		K _L = 0.0165	Chang and Chen, 2005
	GA- (Fe ₃ O ₄)	5.1	200	38.5 mg g ⁻¹		K _L = 0.012	Banerjee and Chen, 2007
	PLCy – (γ-Fe ₂ O ₃)	7 (4 – 9)	1	43.3 mg g ⁻¹	60	-	White et al., 2009
Cd (II)	C-β- C - (Fe ₃ O ₄)	5.5 – 6	300	27.7 mg g ⁻¹	55.9	K _L = 0.214 K _F = 17.64	Badruddoza et al., 2013
	PLCy – (γ-Fe ₂ O ₃)	7	1	43.3 mg g ⁻¹	71	-	White et al., 2009

		(4 – 9)					
Cr(III)	Ce-(Fe ₃ O ₄)	-	0 – 100 100 – 200	25 mg g ⁻¹	35 25	-	Zhu et al., 2011
Cr (VI)	Ch- (Cu ⁰)	4.85	5 50	3.96 mg g ⁻¹ 47.8 mg g ⁻¹		-	Wu et al, 2009
Mn(II)	Ce-(Fe ₃ O ₄)	-	0 – 100 100 – 200	33 mg g ⁻¹	46 33	-	Zhu et al., 2011
Ni(II)	C-β- CD - (Fe ₃ O ₄)	5.5 – 6	300	13.2 mg g ⁻¹	24.3	K _L = 0.043 K _F = 2.39	Badruddoza et al., 2013
	Ch- (Fe ₃ O ₄)	6 (4 – 6)	70 (50-80)	52.55 mg g ⁻¹	> 75	K _L = 1.3448	Tran et al., 2010
	PLCy – (γ-Fe ₂ O ₃)	7 (4 – 9)	1	32.8 mg g ⁻¹	89	-	White et al., 2009
Pb (II)	CA-(γ-Fe ₂ O ₃)	4.7 (1 - 6)	51.8 – 4972.8 1502.2	97.4 mg g ⁻¹		K _L = 0.076	Bèe et al, 2011
	Ce-(Fe ₃ O ₄)		0 – 100 100 – 200	65 mg g ⁻¹ 52 mg g ⁻¹	90 65	-	Zhu et al., 2011
	Ch- (Fe ₃ O ₄)	6 (4 – 6)	70 (50 – 80)	63.33 mg g ⁻¹	> 90	K _L = 0.1097	Tran et al., 2010
	C-β- CD - (Fe ₃ O ₄)	5.5 – 6	200	52.20 mg g ⁻¹		K _L = 0.208 K _F = 16.43	Badruddoza et al., 2012
	C-β- CD - (Fe ₃ O ₄)	5.5 – 6	300	64.5 mg g ⁻¹	99.5	K _L = 0.417 K _F = 25.82	Badruddoza et al., 2013
	PLCy – (γ-Fe ₂ O ₃)	7 (4 – 9)	1	14.7 mg g ⁻¹	67	-	White et al., 2009
Zn	PLCy – (γ-Fe ₂ O ₃)	7 (4 – 9)	1	24.1 mg g ⁻¹	50	-	White et al., 2009

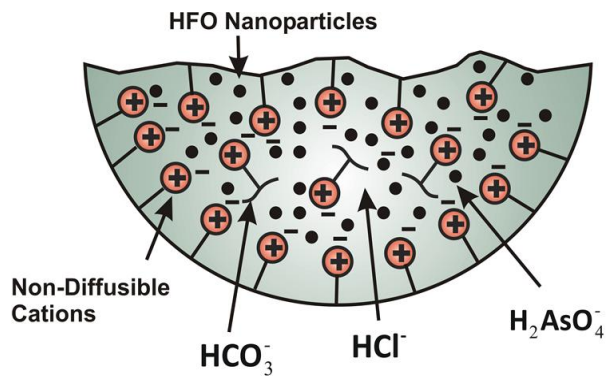


1
2
3
4

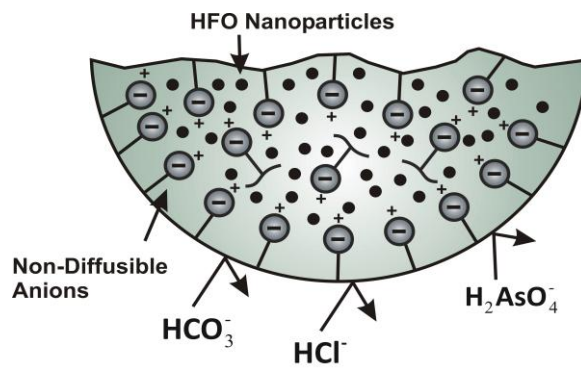
Figure 1 Fabrication methods of PFNCs

1 **Figure 2** Schematic representations of the polymeric cation and anion exchangers used on the
2 S-PFNCs HFO - Hydrated iron (III) oxide. (Modified from Cumbal and Sengupta, 2005).

3



4



5

6